Weak-Memory Dynamics in Discrete Time

Hugues Meyer and Kay Brandner
School of Physics and Astronomy, University of Nottingham, Nottingham NG7 2RD, United Kingdom
and Centre for the Mathematics and Theoretical Physics of Quantum Non-Equilibrium Systems, University of Nottingham, Nottingham NG7 2RD, United Kingdom

(Received 5 November 2025; accepted 20 April 2026; published 1 June 2026)

Discrete dynamics arise naturally in systems with broken temporal translation symmetry and are typically described by first-order recurrence relations representing classical or quantum Markov chains. When memory effects induced by hidden degrees of freedom are relevant, however, higher-order discrete evolution equations are generally required. Focusing on linear dynamics, we identify a well-delineated weak-memory regime where such equations can, on an intermediate timescale, be systematically reduced to a unique first-order counterpart acting on the same state space. We formulate our results as a mathematical theorem and work out two examples showing how they can be applied to stochastic Floquet dynamics under coarse-grained and quantum collisional models.

DOI: 10.1103/kdhy-66b6

The dynamical principles of classical and quantum mechanics imply that physical systems across all scales evolve continuously in time. Nonetheless, processes with broken temporal translation symmetry can often be naturally understood as sequences of discrete steps. Isolated systems subject to rapidly oscillating fields, for example, admit a stroboscopic description in terms of time-independent effective Floquet Hamiltonians that can be engineered through the applied driving, making it possible to realize phenomena with no equilibrium counterparts [1–3]. In open systems, periodic driving typically leads to the formation of limit cycles, where state variables converge to stable fixed points in stroboscopic time [4–7]. This behavior arises from dissipation balancing energy absorption and can be observed, for instance, in mesoscopic devices such as stochastic pumps, which generate directed currents through cyclic variations of control parameters [8–12]; see Fig. 1.

Besides arising naturally from periodic modulations of continuous dynamics, discrete evolution equations also serve as powerful tools to disentangle the complexity of systems with large numbers of interacting degrees of freedom. Discrete-time lattice models, such as cellular automata and quantum circuits, for instance, offer elegant frameworks to explore how macroscopic features of many-body systems such as entanglement spreading and hydrodynamic behavior emerge from local interactions [13–26]. In a similar spirit, collisional models enable an elegant description of open quantum systems, even beyond the weak-coupling regime, by replacing continuous environments with discrete collections of ancillae that interact sequentially with the observable system [27–31]; see Fig. 1.

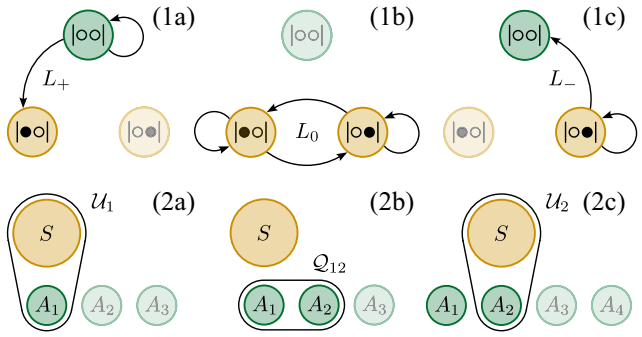


FIG. 1. Top: mesoscopic charge pump. The device consists of two quantum dots, each coupled to a thermochemical reservoir, and admits three microstates corresponding to the left dot, right dot, or neither being occupied. Charge pumping proceeds in a three-stroke cycle: a particle is absorbed by the left dot (1a), tunnels between the dots (1b), and is ejected from the right dot (1c), with respective probabilities L_+, L_0, and L_-. An observer that measures the total charge of the system distinguishes two mesostates whose dynamics are non-Markovian. Bottom: collisional model with memory. A quantum system S interacts sequentially with a stream of identical ancillae A_i. Ancilla A_1 first collides with the system (2a), then with A_2 (2b), before leaving the scattering region (2c). System-ancilla and ancilla-ancilla interactions are described by bipartite maps $\mathcal{U}_i$ and $\mathcal{Q}_{ij}$, respectively.

Published by the American Physical Society under the terms of the Creative Commons Attribution 4.0 International license. Further distribution of this work must maintain attribution to the author(s) and the published article's title, journal citation, and DOI.

A prototypical discrete evolution equation is

$$X_{n+1} = \mathsf{V} X_n, \tag{1}$$

where the vector $X_n \in \mathbb{C}^N$ characterizes the state of the system after n time steps, for example, in terms of a probability distribution, and $\mathsf{V} \in \mathbb{C}^{N\times N}$ is the one-step propagator or generator. Such first-order recurrence relations provide suitable models for systems whose future is, at any point in time, fully determined by their present state. This condition is satisfied if all relevant degrees of freedom are accessible to the observer. In particular in mesoscopic systems, however, it is typically possible to resolve only coarse-grained variables, while details of internal and environmental structures remain inaccessible [32–51]. These hidden degrees of freedom can, if they evolve sufficiently slowly, retain information about the observable system over several time steps while constantly influencing its dynamics. Accounting for this effect requires more general evolution equations of the form

$$X_{n+1} = \mathsf{V} X_n + \sum_{m=1}^{n} \mathsf{K}_m X_{n-m}, \tag{2}$$

where the memory kernel K_n can be either extracted from experimental or simulation data or derived by projecting the state space of a microscopic model onto a lower-dimensional space of mesostates [52–58]. We assume throughout that neither the one-step propagator nor the memory kernel depend explicitly on time. This condition is satisfied whenever the underlying microdynamics are stroboscopically homogeneous, as is the case for stationary and periodically driven processes.

Higher-order recurrence relations of the type of Eq. (2) can provide significantly more accurate models for systems with hidden degrees of freedom than their first-order counterparts, especially when high temporal resolution is required, and memory effects cannot be suppressed by controlling the time step. However, they are also less physically transparent and more difficult to solve both analytically and numerically, especially when the accessible state space remains large. Here, we show how this trade-off can be systematically overcome in settings where memory effects play a subdominant role. To this end, we reconstruct a recently developed theory of continuous weak memory in discrete time, thereby substantially broadening the scope of this framework [59,60].

The key idea of our approach is to construct an effective generator $\mathsf{G} \in \mathbb{C}^{N\times N}$ such that the solution $Y_n \in \mathbb{C}^N$ of the first-order recurrence relation

$$Y_{n+1} = \mathsf{G} Y_n \tag{3}$$

converges to the solution of Eq. (2) at sufficiently long times. The short-time dynamics of the system are described as an effectively instantaneous change in its initial state, $Y_0 = \mathsf{D} X_0$, induced by the slippage matrix $\mathsf{D} \in \mathbb{C}^{N\times N}$, which, for any X_0, has to satisfy

$$\lim_{n\to\infty} \mathsf{G}^{-n} X_n = \mathsf{D} X_0. \tag{4}$$

Here, G and D must be nonsingular to ensure that the long-time approximation Y_n is nontrivial for any $X_0 \neq 0$. The physical intuition behind this ansatz is that, after a brief transient period, all hidden degrees of freedom reach a near-stationary state, which then evolves almost adiabatically under the influence of the observable ones. As a result, the backflow of information from inaccessible to accessible components of the system gradually diminishes and the impact of memory effects becomes insignificant.

The validity of this picture depends on three characteristic timescales, which we define by imposing the bounds

$$\|\mathsf{V}^{-1}\| \leq 1/v, \qquad \|\mathsf{K}_n\| \leq M k^{n-1} \tag{5}$$

on the free generator and the memory kernel, where $\|\cdot\|$ denotes the spectral norm. Here, v corresponds to the slowest mode of the adiabatic dynamics, which would be observed if the evolution of all hidden degrees of freedom was frozen. The parameters M and $k < 1$ quantify, respectively, the coupling strength between accessible and inaccessible parts of the system and the relaxation rate of the latter. Thus, when M and k are small compared to v, the hidden degrees of freedom evolve nearly autonomously, with the observable ones acting only as a weak and slow perturbation. Under these conditions, memory effects are expected to be subdominant, and an effective generator satisfying Eq. (4) may exist.

Our main achievement is to translate the qualitative analysis above into a mathematical theorem, which can be formulated as follows. If the parameters v, M, and k entering the bounds in Eq. (5) satisfy

$$k < v, \qquad M < M^* = \begin{cases} (v-k)^2/4, & v+k<2 \\ (1-k)(v-1), & v+k\geq 2 \end{cases}, \tag{6}$$

there exists a unique effective generator G such that, for any initial state X_0, the long-time approximation Y_n of the solution X_n of Eq. (2) satisfies

$$|X_n - Y_n| \leq \frac{\zeta - k}{\eta - \zeta} |X_0| \zeta^n \tag{7}$$

with

$$\zeta = (v+k)/2 - \sqrt{(v-k)^2/4 - M} < 1, \tag{8}$$

$$\eta = (v+k)/2 + \sqrt{(v-k)^2/4 - M}, \tag{9}$$

and $|\cdot|$ indicating the Euclidean norm. The corresponding slippage matrix is given by the formula

$$\mathsf{D}^{-1} = 1 + \sum_{m=1}^{\infty}\sum_{n=1}^{\infty} \mathsf{H}^{-m}\mathsf{K}_{m+n-1}\mathsf{G}^{-n}, \tag{10}$$

where G and H are the unique solutions of the fixed-point equations

$$\mathsf{G} = \mathsf{V} + \sum_{n=1}^{\infty} \mathsf{K}_n \mathsf{G}^{-n} = T(\mathsf{G}), \tag{11}$$

$$\mathsf{H} = \mathsf{V} + \sum_{n=1}^{\infty} \mathsf{H}^{-n}\mathsf{K}_n = U(\mathsf{H}) \tag{12}$$

in the set $B = \{\mathsf{X} \in \mathbb{C}^{N\times N} : \|\mathsf{X}^{-1}\| \leq 1/\eta\}$.

The proof of this theorem and the required mathematical methods are discussed in Supplemental Material [61]. Here, we add only three remarks. First, Eqs. (5) and (6) define the weak-memory regime for discrete dynamics, where our theory is applicable without further restrictions. These conditions do not require a strong separation of timescales, but can be met even when M, k, and v are of the same order of magnitude. In such situations, phenomenological methods such as the standard Born-Markov approximation are typically not reliable [66–70].

Second, Eq. (7) provides a strong bound on the error of the long-time approximation, thereby enforcing the uniqueness of the effective generator. That is, while there may exist a whole family of generators that define a nonsingular slippage matrix, there is only one such pair whose corresponding long-time approximation satisfies

$$\lim_{n\to\infty} |X_n - Y_n|\zeta^{-n} < \infty \tag{13}$$

for any X_0. Finally, Eqs. (10)–(12) provide an explicit scheme to construct this optimal approximation to arbitrary accuracy, which would not be possible with standard weak-coupling expansions whose convergence properties are not generally understood. To this end, the fixed-point equations (11) and (12) may be solved with a suitable ansatz or by iteration, where the latter approach exploits the fact that T and U are contractions on B under the metric $d(\mathsf{X},\mathsf{Y}) = \|\mathsf{X}-\mathsf{Y}\|$.

As a first application, we show how theory can be employed in the coarse graining of Markov processes. We focus on systems with a finite space of microstates $\mathbb{M} = \{1,\ldots,M\}$ and denote by $P_n = [P_n^1,\ldots,P_n^M]$ the time dependent vector that assigns an occupation probability to every microstate. Dynamics are governed by the discrete-time master equation $P_{n+1} = \mathsf{L}P_n$, where $(\mathsf{L})_{ij} \geq 0$ is the probability to transition from the microstates i to the microstate j in one step. A coarse graining is induced by a partitioning of $\mathbb{M}$ into N disjoint subsets $\mathbb{M}_\alpha$, which correspond to the operationally distinguishable configurations of the system. The occupation probabilities $X_n^\alpha = \sum_{i\in\mathbb{M}_\alpha} P_n^i$ of these mesostates are collected in the lumped vector $X_n = [X_n^1,\ldots,X_n^N]$. Under minor technical conditions, this vector follows an evolution equation of the form of Eq. (2), where V and K_n can be expressed in terms of the microscopic transition matrix L using projection operator techniques [55–58].

Our master theorem extends this framework by establishing rigorous conditions for the existence of, and systematic procedures to construct, an effective generator of the lumped dynamics. These results apply to broad classes of physical systems, including, in particular, ones with continuous underlying dynamics. Systems such as electronic nanodevices, for example, are typically described by a continuous-time master equation [71,72], $\dot{p}_t = \mathsf{W}_t p_t$. Here, $p_t = [p_t^1,\ldots,p_t^M]^\mathsf{T}$ is a vector of occupation probabilities; $(\mathsf{W}_t)_{ij} \geq 0$ is the transition rate from the microstate j to the microstate i, which becomes time dependent under external driving; and $(\mathsf{W}_t)_{ii} = -\sum_{j\neq i}(\mathsf{W}_t)_{ji}$ to ensure probability conservation. If the driving is periodic, $\mathsf{W}_{t+\tau} = \mathsf{W}_t$, Floquet's theorem implies that the stroboscopic vector $P_n = p_{n\tau}$ follows a discrete-time master equation with the transition matrix $\mathsf{L} = \exp_{\mathrm{O}}[\int_0^\tau dt \mathsf{W}_t]$. This observation shows that our theory opens a path to systematically derive effective generators for coarse-grained, periodically modulated dynamics, a task that could not be addressed with the existing weak-memory theory for continuous dynamics, and, more generally, poses a significant challenge without additional assumptions on the driving timescale or the use of uncontrolled approximations [73–77].

Two remarks are in order before we move on to a simple example. First, if L is a stochastic matrix, as assumed above, then so is the free generator V of the lumped dynamics. Consequently, the Perron-Frobenius theorem implies $v \leq 1$ for this entire class of models. Second, while we have so far focused on classical Markov jump processes, our conclusions extend directly to open quantum systems with a finite-dimensional Hilbert space upon replacing probability vectors, transition matrices, and rate matrices by density matrices, quantum channels, and Lindblad generators, respectively.

We now focus on the charge-pump model of Fig. 1. A complete operation cycle consists of the three strokes shown in panels (a), (b), and (c), which are described by the stochastic matrices L_+, L_0, L_-, respectively. The microscopic transition matrix is given by $\mathsf{L} = \mathsf{L}_-\mathsf{L}_0\mathsf{L}_+$. For an observer monitoring only the total charge of the two quantum dots, the system is described by the lumped probability vector $X_n = [X_n^\circ, X_n^\bullet]^\mathsf{T}$, where $X_n^\circ = P_n^{\circ\,\circ}$ and $X_n^\bullet = P_n^{\circ\,\bullet} + P_n^{\bullet\,\circ}$. If the initial charge distribution is symmetric, as we assume here only for the sake of simplicity, $P_0^{\circ\,\bullet} = P_0^{\bullet\,\circ}$, this vector follows Eq. (2) with

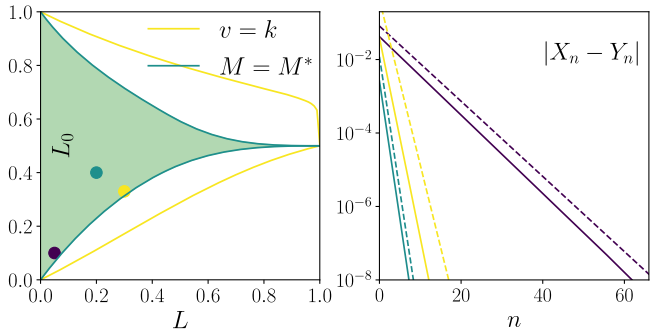


FIG. 2. Mesoscopic charge pump. Left: for $L_+ = L_- = L$, the shaded area indicates the region in the parameter space of the model, where the weak-memory conditions, Eqs. (5) and (6), are satisfied with $v = 1/\|\mathsf{V}^{-1}\|$ and $M = \|\mathsf{K}_1\|$. Right: error of the long-time approximation $Y_n = \mathsf{G}^n\mathsf{D}X_0$ with respect to the exact solution X_n of Eq. (2) (solid), for $X_0 = [1, 0]^\mathsf{T}$ and selected parameter sets, indicated with dots in the left panel. For comparison, we also show the error bound [Eq. (7)] (dashed).

$$\mathsf{V} = 1 + L_+(1 - L_0L_-)\mathsf{J}_1 + \frac{L_-}{2}\mathsf{J}_2, \tag{14}$$

$$\mathsf{K}_n = \frac{L_+L_-(1 - 2L_0 + 2L_-)k^n}{2 - L_-}\mathsf{J}_1 - \frac{L_-^2k^n}{2(2 - L_-)}\mathsf{J}_2, \tag{15}$$

where $k = (1 - 2L_0)(2 - L_-)/2$; $\mathsf{J}_1 = \left[\begin{smallmatrix}-1 & 0\\ 1 & 0\end{smallmatrix}\right]$; $\mathsf{J}_2 = \left[\begin{smallmatrix}0 & 1\\ 0 & -1\end{smallmatrix}\right]$; and L_+, L_0, and L_- are the absorption, tunneling, and ejection probabilities as defined in Fig. 1. For $L_0 = 1/2$, the charge distribution fully equilibrates in one cycle, and the memory kernel vanishes. Away from this limit, the parameters $L_\pm$, which are determined by the coupling strengths between quantum dots and reservoirs, must remain sufficiently small for the weak-memory conditions in Eqs. (5) and (6) to hold; see Fig. 2. In this regime, the fixed-point equation (11) for the effective generator can be solved using the ansatz $\mathsf{G} = 1 + g_1\mathsf{J}_1 + g_2\mathsf{J}_2$, and the adjoint generator H follows analogously. The long-time approximation $Y_n = \mathsf{G}^n\mathsf{D}X_0$ is then obtained using the formula in Eq. (10) for the slippage matrix D [61]. As Fig. 2 shows, the error of this approximation decays exponentially with n, closely following the upper bound [Eq. (7)].

As our second main application, we consider collisional models, which offer a versatile platform to describe open or monitored quantum dynamics in discrete time [78]. As illustrated in Fig. 1, such models consist of a system of interest that couples sequentially to a collection of identical environmental units, or ancillae. Memory effects can be added to this framework, for instance, through interactions between successive ancillae. The state of the system after n collisions is then given by

$$\rho_n = \mathrm{Tr}_A\left[\mathcal{U}_n \cdots \mathcal{U}_2\mathcal{Q}_{12}\mathcal{U}_1(\rho_0 \otimes \xi^n)\right], \tag{16}$$

where $\xi^n = \bigotimes_{i=1}^n \xi_i$ is the initial state of the ancillae, and $\mathrm{Tr}_A[\circ]$ indicates the partial trace over their joint Hilbert space. The maps $\mathcal{U}_i$ and $\mathcal{Q}_{ij}$ describe bipartite interactions between the ith ancilla and the system and between the ith and the jth ancillae, respectively.

For concreteness, we now assume that the system and the ancillae are qubits with ground and excited states $|0_i\rangle$ and $|1_i\rangle$, where $i = S, 1, \ldots, n$. System-ancilla and ancilla-ancilla interactions are described as unitary and incoherent partial swaps,

$$\mathcal{U}_i \circ = \mathsf{U}_i \circ \mathsf{U}_i^\dagger, \qquad \mathcal{Q}_{ij} \circ = (1 - k) \circ + k\mathsf{S}_{ij} \circ \mathsf{S}_{ij}, \tag{17}$$

where $\mathsf{U}_i = \sqrt{1 - u} - \mathrm{i}\sqrt{u}\mathsf{S}_{Si}$ and $0 < u, k < 1$. The swap matrices are defined such that $\mathsf{S}_{ij}|\alpha_i, \beta_j\rangle = |\beta_i, \alpha_j\rangle$ for $\alpha, \beta \in \{0, 1\}$. If all ancillae are initially prepared in the same state, the dynamics of this model are governed by the recursion relation

$$\rho_{n+1} = \mathcal{K}_0\rho_n + \sum_{m=1}^n \mathcal{K}_m\rho_{n-m} + \mathcal{F}_{n+1}\rho_0, \tag{18}$$

with $\mathcal{K}_n = (1/k - 1)\mathcal{F}_{n+1}$ and $\mathcal{F}_n \circ = k^n\mathrm{Tr}_1 \times [\mathcal{U}_1^n(\circ \otimes \xi_1)]$; see Refs. [61,78]. Since $\mathcal{F}_n$ is a linear map on the operator space of the system, it can be represented as a four-dimensional matrix [79]. Thus, Eq. (18) has the structure of Eq. (2), up to an inhomogeneous term, which can, however, be accounted for. If $\mathcal{G}$ and $\mathcal{D}$ are the effective generator and slippage map of the homogeneous dynamics, then the long-time approximation of ρ_n reads [61]

$$\chi_n = \mathcal{G}^n\mathcal{D}\rho_0 + \sum_{m=1}^n \mathcal{G}^{n-m}\mathcal{D}\mathcal{F}_m\rho_0. \tag{19}$$

To evaluate this expression, we solve the fixed-point equations (11) and (12) numerically by iteration using the initial guesses $\mathcal{G}_0 = \mathcal{H}_0 = \mathcal{K}_0$; the corresponding slippage map then follows from Eq. (10). As we show in Fig. 3, the error of the resulting approximations first decays exponentially with time, obeying the bound

$$|\rho_n - \chi_n| \le \frac{\zeta - k}{\eta - \zeta}|\rho_0|\zeta^n\left(1 + \sum_{m=1}^n \|\mathcal{F}_m\|\zeta^{-m}\right), \tag{20}$$

which follows from Eq. (7) and holds for the exact effective generator and slippage map [61], before approaching a plateau whose value decreases exponentially with the number of iterations used to determine the generator.

This observation shows that iterating the fixed-point equations (11) and (12) provides an efficient numerical method for determining the effective generator and the associated slippage matrix. However, due to their nonlinear structures, these equations generally do not provide a convenient starting point for analytical perturbation

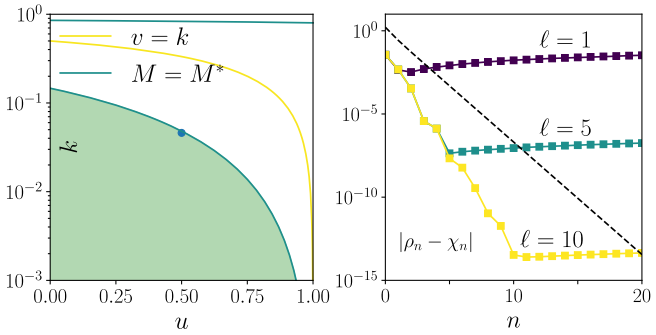


FIG. 3. Collisional model. Left: weak-memory regime in the parameter space defined by the swap probabilities u and k, with $v = (1-u)(1-k)$ and $M = k(1-k)$. The ancillae are initially in fully mixed states. Right: error of the long-time approximation [Eq. (19)] for different approximate generators $\mathcal{G}_\ell = T(\mathcal{G}_{\ell-1})$ (solid) together with the bound [Eq. (20)] (dashed). For all plots, we used the model parameters indicated by the dot in the left panel and set $\rho_0 = |0_S\rangle\langle 0_S|$.

schemes. For this purpose, it is more instructive to focus instead on the $\mathsf{E}_n \in \mathbb{C}^{N\times N}$, which, for any given G, is uniquely defined by requiring that the inhomogeneous recurrence relation

$$X_{n+1} = \mathsf{G}X_n + \mathsf{E}_n X_0 \tag{21}$$

is equivalent to Eq. (2). If the weak-memory conditions, Eqs. (5) and (6), are fulfilled, and G is the optimal effective generator of our master theorem, this function satisfies the linear summation equation

$$\mathsf{E}_n = -\sum_{m=n+1}^{\infty}\left(\mathsf{K}_m + \sum_{l=1}^{m-1}\mathsf{E}_{l-1}\mathsf{K}_{m-l}\right)\mathsf{V}^{n-m}, \tag{22}$$

which can be solved by iteration. In this way, the optimal memory function E_n of a given model can be systematically constructed from an initial guess E_n^0. This initial guess may either be set to zero or derived from an exact solution of Eq. (2) for a suitable limiting case of the model. If the free solution satisfies the bound $\|\mathsf{E}_n^0\| \leq S\sigma^n$ with $\zeta \leq \sigma < \min\{\eta, 1\}$ and $S \geq \sigma - k$, the iteration converges. Once the optimal memory function has been determined, the corresponding effective generator and slippage matrix follow from the relations

$$\mathsf{G} = \mathsf{V} - \mathsf{E}_0, \qquad \mathsf{D} = 1 + \sum_{n=1}^{\infty}\mathsf{G}^{-n}\mathsf{E}_{n-1}. \tag{23}$$

For the trivial initial guess $\mathsf{E}_n^0 = 0$, for instance, we obtain an expansion of G in powers of the coupling strength M.

These results, whose derivation we provide in Ref. [61], complete our theory of weak memory effects in discrete time. Before closing, we stress that, while the above framework achieves a high degree of structural uniformity with the one recently developed for continuous dynamics, our results could not be derived from that theory, since the exact discretization of evolution equations with memory is a nontrivial procedure. In particular, there is no simple correspondence between the discrete one-step propagator and memory kernel and their continuous counterparts. More generally, our Letter provides a universal basis to explore the potentially rich physics of dynamical memory in settings with inherently discrete dynamics, such as many-body circuit and collisional models. On the applied side, it offers new tools for the extrapolation of short-time data obtained from experiments or molecular dynamics simulations [80–85]. The applicability of our framework is determined solely by the weak-memory conditions in Eqs. (5) and (6). It thus extends beyond the standard weak-coupling and quasi-Markovian limits, which impose stronger and less rigorous constraints on system parameters. At the same time, our results provide a well-defined starting point for future research seeking to systematically characterize strong-memory dynamics.

Acknowledgments—This work was supported by the Medical Research Council (Grants No. MR/S034714/1 and No. MR/Y003845/1) and the Engineering and Physical Sciences Research Council (Grant No. EP/V031201/1).

Data availability—The data are not publicly available. The data are available from the authors upon reasonable request.

[1] M. Bukov, L. D'Alessio, and A. Polkovnikov, Universal high-frequency behavior of periodically driven systems: From dynamical stabilization to Floquet engineering, Adv. Phys. **64**, 139 (2015).
[2] A. Eckardt, Colloquium: Atomic quantum gases in periodically driven optical lattices, Rev. Mod. Phys. **89**, 011004 (2017).
[3] T. Oka and S. Kitamura, Floquet engineering of quantum materials, Annu. Rev. Condens. Matter Phys. **10**, 387 (2019).
[4] M. Moskalets and M. Büttiker, Floquet scattering theory of quantum pumps, Phys. Rev. B **66**, 205320 (2002).
[5] S. Ray and A. C. Barato, Stochastic thermodynamics of periodically driven systems: Fluctuation theorem for currents and unification of two classes, Phys. Rev. E **96**, 052120 (2017).
[6] P. Menczel and K. Brandner, Limit cycles in periodically driven open quantum systems, J. Phys. A **52**, 43LT01 (2019).
[7] T. Mori, Floquet states in open quantum systems, Annu. Rev. Condens. Matter Phys. **14**, 35 (2023).
[8] N. A. Sinitsyn and I. Nemenman, Universal geometric theory of mesoscopic stochastic pumps and reversible ratchets, Phys. Rev. Lett. **99**, 220408 (2007).

[9] S. Rahav, J. Horowitz, and C. Jarzynski, Directed flow in nonadiabatic stochastic pumps, Phys. Rev. Lett. **101**, 140602 (2008).
[10] M. Esposito and J. M. R. Parrondo, Stochastic thermodynamics of hidden pumps, Phys. Rev. E **91**, 052114 (2015).
[11] O. Raz, Y. Subaşı, and C. Jarzynski, Mimicking nonequilibrium steady states with time-periodic driving, Phys. Rev. X **6**, 021022 (2016).
[12] K. Funo, N. Lambert, F. Nori, and C. Flindt, Shortcuts to adiabatic pumping in classical stochastic systems, Phys. Rev. Lett. **124**, 150603 (2020).
[13] A. Nahum, J. Ruhman, S. Vijay, and J. Haah, Quantum entanglement growth under random unitary dynamics, Phys. Rev. X **7**, 031016 (2017).
[14] A. Nahum, S. Vijay, and J. Haah, Operator spreading in random unitary circuits, Phys. Rev. X **8**, 021014 (2018).
[15] C. W. Von Keyserlingk, T. Rakovszky, F. Pollmann, and S. L. Sondhi, Operator hydrodynamics, OTOCs, and entanglement growth in systems without conservation laws, Phys. Rev. X **8**, 021013 (2018).
[16] V. Khemani, A. Vishwanath, and D. A. Huse, Operator spreading and the emergence of dissipative hydrodynamics under unitary evolution with conservation laws, Phys. Rev. X **8**, 031057 (2018).
[17] A. Chan, A. De Luca, and J. T. Chalker, Solution of a minimal model for many-body quantum chaos, Phys. Rev. X **8**, 041019 (2018).
[18] T. Rakovszky, F. Pollmann, and C. W. Von Keyserlingk, Diffusive hydrodynamics of out-of-time-ordered correlators with charge conservation, Phys. Rev. X **8**, 031058 (2018).
[19] T. Rakovszky, F. Pollmann, and C. W. Von Keyserlingk, Sub-ballistic growth of Rényi entropies due to diffusion, Phys. Rev. Lett. **122**, 250602 (2019).
[20] B. Bertini, P. Kos, and T. Prosen, Entanglement spreading in a minimal model of maximal many-body quantum chaos, Phys. Rev. X **9**, 021033 (2019).
[21] K. Klobas, B. Bertini, and L. Piroli, Exact thermalization dynamics in the "rule 54" quantum cellular automaton, Phys. Rev. Lett. **126**, 160602 (2021).
[22] K. Klobas and B. Bertini, Entanglement dynamics in rule 54: Exact results and quasiparticle picture, SciPost Phys. **11**, 107 (2021).
[23] K. Klobas and B. Bertini, Exact relaxation to Gibbs and non-equilibrium steady states in the quantum cellular automaton rule 54, SciPost Phys. **11**, 106 (2021).
[24] B. Buča, K. Klobas, and T. Prosen, Rule 54: Exactly solvable model of nonequilibrium statistical mechanics, J. Stat. Mech. (2021) P074001.
[25] B. Bertini, C. De Fazio, J. P. Garrahan, and K. Klobas, Exact quench dynamics of the Floquet quantum east model at the deterministic point, Phys. Rev. Lett. **132**, 120402 (2024).
[26] S. W. P. Kim, F. Hübner, J. P. Garrahan, and B. Doyon, Circuits as a simple platform for the emergence of hydrodynamics in deterministic chaotic many-body systems, arXiv:2503.08788.
[27] D. Karevski and T. Platini, Quantum nonequilibrium steady states induced by repeated interactions, Phys. Rev. Lett. **102**, 207207 (2009).
[28] P. Strasberg, G. Schaller, T. Brandes, and M. Esposito, Quantum and information thermodynamics: A unifying framework based on repeated interactions, Phys. Rev. X **7**, 021003 (2017).
[29] P. Strasberg, Repeated interactions and quantum stochastic thermodynamics at strong coupling, Phys. Rev. Lett. **123**, 180604 (2019).
[30] S. Seah, S. Nimmrichter, D. Grimmer, J. P. Santos, V. Scarani, and G. T. Landi, Collisional quantum thermometry, Phys. Rev. Lett. **123**, 180602 (2019).
[31] F. L. S. Rodrigues, G. De Chiara, M. Paternostro, and G. T. Landi, Thermodynamics of weakly coherent collisional models, Phys. Rev. Lett. **123**, 140601 (2019).
[32] S. Pigolotti and A. Vulpiani, Coarse graining of master equations with fast and slow states, J. Chem. Phys. **128**, 154114 (2008).
[33] M. Esposito, Stochastic thermodynamics under coarse graining, Phys. Rev. E **85**, 041125 (2012).
[34] R. Yvinec, C. Zhuge, J. Lei, and M. C. Mackey, Adiabatic reduction of a model of stochastic gene expression with jump Markov process, J. Math. Biol. **68**, 1051 (2014).
[35] G. Hummer and A. Szabo, Optimal dimensionality reduction of multistate kinetic and Markov-state models, J. Phys. Chem. B **119**, 9029 (2015).
[36] A. Wachtel, R. Rao, and M. Esposito, Thermodynamically consistent coarse graining of biocatalysts beyond Michaelis–Menten, New J. Phys. **20**, 042002 (2018).
[37] A. Lapolla and A. Godec, Manifestations of projection-induced memory: General theory and the tilted single file, Front. Phys. **7**, 182 (2019).
[38] P. Strasberg and M. Esposito, Non-Markovianity and negative entropy production rates, Phys. Rev. E **99**, 012120 (2019).
[39] D. M. Busiello, D. Gupta, and A. Maritan, Coarse-grained entropy production with multiple reservoirs: Unraveling the role of time scales and detailed balance in biology-inspired systems, Phys. Rev. Res. **2**, 043257 (2020).
[40] D. Seiferth, P. Sollich, and S. Klumpp, Coarse graining of biochemical systems described by discrete stochastic dynamics, Phys. Rev. E **102**, 062149 (2020).
[41] S. A. M. Loos and S. H. L. Klapp, Irreversibility, heat and information flows induced by non-reciprocal interactions, New J. Phys. **22**, 123051 (2020).
[42] A. V. Straube, B. G. Kowalik, R. R. Netz, and F. Höfling, Rapid onset of molecular friction in liquids bridging between the atomistic and hydrodynamic pictures, Commun. Phys. **3**, 126 (2020).
[43] C. Ayaz, L. Tepper, F. N. Brünig, J. Kappler, J. O. Daldrop, and R. R. Netz, Non-Markovian modeling of protein folding, Proc. Natl. Acad. Sci. U.S.A. **118**, e2023856118 (2021).
[44] D. Hartich and A. Godec, Emergent memory and kinetic hysteresis in strongly driven networks, Phys. Rev. X **11**, 041047 (2021).
[45] A. Lapolla and A. Godec, Toolbox for quantifying memory in dynamics along reaction coordinates, Phys. Rev. Res. **3**, L022018 (2021).
[46] D. Hartich and A. Godec, Violation of local detailed balance upon lumping despite a clear timescale separation, Phys. Rev. Res. **5**, L032017 (2023).

[47] F. Coghi, Current fluctuations of a self-interacting diffusion on a ring, J. Phys. A **58**, 015002 (2024).

[48] K. Blom, K. Song, E. Vouga, A. Godec, and D. E. Makarov, Milestoning estimators of dissipation in systems observed at a coarse resolution, Proc. Natl. Acad. Sci. U.S.A. **121**, e2318333121 (2024).

[49] L. Vollmar, R. Bebon, J. Schimpf, B. Flietel, S. Celiksoy, C. Sönnichsen, A. Godec, and T. Hugel, Model-free inference of memory in conformational dynamics of a multi-domain protein, J. Phys. A **57**, 365001 (2024).

[50] X. Zhao, D. Hartich, and A. Godec, Emergence of memory in equilibrium versus nonequilibrium systems, Phys. Rev. Lett. **132**, 147101 (2024).

[51] M. Wiśniewski and J. Spiechowicz, Memory-induced current reversal of Brownian motors, Phys. Rev. E **111**, 024130 (2025).

[52] D. Lesnicki, R. Vuilleumier, A. Carof, and B. Rotenberg, Molecular hydrodynamics from memory kernels, Phys. Rev. Lett. **116**, 147804 (2016).

[53] G. Jung, M. Hanke, and F. Schmid, Iterative reconstruction of memory kernels, J. Chem. Theory Comput. **13**, 2481 (2017).

[54] H. Meyer, S. Wolf, G. Stock, and T. Schilling, A numerical procedure to evaluate memory effects in non-equilibrium coarse-grained models, Adv. Theor. Simul. **4**, 2000197 (2021).

[55] M. T. Vrugt and R. Wittkowski, Projection operators in statistical mechanics: A pedagogical approach, Eur. J. Phys. **41**, 045101 (2020).

[56] V. Klippenstein, M. Tripathy, G. Jung, F. Schmid, and N. F. A. Van Der Vegt, Introducing memory in coarse-grained molecular simulations, J. Phys. Chem. B **125**, 4931 (2021).

[57] T. Schilling, Coarse-grained modelling out of equilibrium, Phys. Rep. **972**, 1 (2022).

[58] B. Hilder and U. Sharma, Quantitative coarse-graining of Markov chains, SIAM J. Math. Anal. **56**, 913 (2024).

[59] K. Brandner, Dynamics of microscale and nanoscale systems in the weak-memory regime, Phys. Rev. Lett. **134**, 037101 (2025).

[60] K. Brandner, Dynamics of microscale and nanoscale systems in the weak-memory regime: A mathematical framework beyond the Markov approximation, Phys. Rev. E **111**, 014137 (2025).

[61] See Supplemental Material at http://link.aps.org/supplemental/10.1103/kdhy-66b6, which provides details of the calculations leading to the results presented in the main text. It is divided in three sections: (i) Master Theorem, (ii) Application 1: Mesoscopic Charge Pump, (iii) Application 2: Collisional Model. It includes Refs. [62–65].

[62] P. Agarwal, M. Jleli, and B. Samet, *Fixed Point Theory in Metric Spaces*, 1st ed. (Springer Nature, Singapore, 2018).

[63] R. A. Horn and C. R. Johnson, *Matrix Analysis*, 2nd ed. (Cambridge University Press, New York, NY, 2013).

[64] Á. Rivas and S. F. Huelga, *Open Quantum Systems: An Introduction*, 1st ed., SpringerBriefs in Physics (Springer, Berlin, Heidelberg, 2012).

[65] T. Burton, *Volterra Integral and Differential Equations*, 2nd ed., Mathematics in Science and Engineering Vol. 202 (Elsevier, Amsterdam, 2005).

[66] W. T. Strunz and T. Yu, Convolutionless non-Markovian master equations and quantum trajectories: Brownian motion, Phys. Rev. A **69**, 052115 (2004).

[67] C. H. Fleming and N. I. Cummings, Accuracy of perturbative master equations, Phys. Rev. E **83**, 031117 (2011).

[68] R. Hartmann and W. T. Strunz, Accuracy assessment of perturbative master equations: Embracing nonpositivity, Phys. Rev. A **101**, 012103 (2020).

[69] C. S. Tello Breuer, T. Becker, and A. Eckardt, Benchmarking quantum master equations beyond ultraweak coupling, Phys. Rev. B **110**, 064319 (2024).

[70] Z. Sartipi, R. Gundermann, J. Anders, and P. Saalfrank, Canonically consistent quantum master equation for proton-transfer reactions, arXiv:2603.21865.

[71] U. Seifert, Stochastic thermodynamics, fluctuation theorems and molecular machines, Rep. Prog. Phys. **75**, 126001 (2012).

[72] G. Benenti, G. Casati, K. Saito, and R. S. Whitney, Fundamental aspects of steady-state conversion of heat to work at the nanoscale, Phys. Rep. **694**, 1 (2017).

[73] E. Mozgunov and D. Lidar, Completely positive master equation for arbitrary driving and small level spacing, Quantum **4**, 227 (2020).

[74] F. Nathan and M. S. Rudner, Universal Lindblad equation for open quantum systems, Phys. Rev. B **102**, 115109 (2020).

[75] A. Schnell, A. Eckardt, and S. Denisov, Is there a Floquet Lindbladian?, Phys. Rev. B **101**, 100301 (2020).

[76] R. Hotz and G. Schaller, Coarse-graining master equation for periodically driven systems, Phys. Rev. A **104**, 052219 (2021).

[77] T. Mori, Strong Markov dissipation in driven-dissipative quantum systems, J. Stat. Phys. **192**, 1 (2025).

[78] F. Ciccarello, S. Lorenzo, V. Giovannetti, and G. M. Palma, Quantum collision models: Open system dynamics from repeated interactions, Phys. Rep. **954**, 1 (2022).

[79] In our discussion of collisional models, we formally treat density matrices as vectors and quantum maps as matrices. For this approach to be consistent, $|\cdot|$ must, when applied to a density matrix, be evaluated as the Hilbert-Schmidt norm; $\|\cdot\|$ denotes the operator norm induced by $|\cdot|$ throughout.

[80] G. Jung, M. Hanke, and F. Schmid, Iterative reconstruction of memory kernels, J. Chem. Theory Comput. **13**, 2481 (2017).

[81] V. Klippenstein, M. Tripathy, G. Jung, F. Schmid, and N. F. A. Van Der Vegt, Introducing memory in coarse-grained molecular simulations, J. Phys. Chem. B **125**, 4931 (2021).

[82] H. Vroylandt, L. Goudenège, P. Monmarché, F. Pietrucci, and B. Rotenberg, Likelihood-based non-Markovian models from molecular dynamics, Proc. Natl. Acad. Sci. U.S.A. **119**, e2117586119 (2022).

[83] L. Tepper, B. Dalton, and R. R. Netz, Accurate memory kernel extraction from discretized time-series data, J. Chem. Theory Comput. **20**, 3061 (2024).

[84] B. A. Dalton, A. Klimek, H. Kiefer, F. N. Brünig, H. Colinet, L. Tepper, A. Abbasi, and R. R. Netz, Memory and friction: From the nanoscale to the macroscale, Annu. Rev. Phys. Chem. **76**, 431 (2025).

[85] S. Satore, F. Teichmann, and G. Stock, Markov-type state models to describe non-Markovian dynamics, J. Chem. Theory Comput. **21**, 2757 (2025).